Received: 16 November 2025 | Revised: 18 March 2026 | Accepted: 29 June 2026 | Published online: 25 August 2026

RESEARCH ARTICLE

Archives of Advanced Engineering Science
2026, Vol. 4(4) 411–422
DOI: 10.47852/bonviewAAES62028258

Asymmetric Configuration for a Four-Motor Omnidirectional Robot

Raimondo Sgrò[1,*] and Sergio Cacciatori[2]

[1] *IIS Cobianchi, Italy*

[2] *Dipartimento di Scienza e Alta Tecnologia, Università degli Studi dell'Insubria, Italy*

Abstract: Four-wheel omnidirectional robots are commonly designed under the assumption of symmetric wheel placement. However, compact platforms and mechanically constrained layouts often require asymmetric configurations, where front and rear wheel angles differ. In such cases, symmetric inverse-kinematics formulations may introduce non-negligible errors. This paper presents an explicit analytical formulation for inverse kinematics in four-wheel omnidirectional robots with arbitrary wheel angles α and β. The derivation is based on a structured linear-algebraic treatment that avoids symmetry assumptions and yields closed-form expressions for motor velocities. The kinematic error introduced by applying symmetric-case equations to asymmetric layouts is analytically quantified. Experimental validation was conducted on a four-wheel omnidirectional robot configured with $\alpha = 55°$ and $\beta = 45°$. Two representative steering angles (15° and 30°) were tested with repeated runs per condition. The proposed formulation showed improved directional accuracy compared to standard symmetric RoboCup-based equations. At 15°, the mean angular error was significantly reduced, while at 30°, the symmetric approximation exhibited a large systematic deviation, with heading errors exceeding 16° on average. Although the current validation is limited to selected configurations, the results demonstrate that asymmetric geometries require dedicated kinematic treatment to ensure motion fidelity. The proposed formulation provides a practical engineering solution for compact omnidirectional robots where symmetry cannot be maintained.

Keywords: omnidirectional movement, inverse kinematics, holonomic robots

1. Introduction

Omnidirectional movement was developed to provide mobile robots with greater agility in confined environments.

Their use continues to expand in autonomous navigation applications, an area that remains the subject of active research [1]. Unlike differential-drive systems, which rely on two powered wheels and impose nonholonomic constraints, omnidirectional platforms are holonomic and allow independent control of planar translation (x, y) and rotation (θ). Omnidirectional mobile robots are widely used in service, industrial, and research applications due to their high maneuverability [2]. Two classical configurations are commonly adopted: a three-wheel layout with wheels spaced 120° apart (often referred to as a Kiwi drive) and a four-wheel layout with drive wheels positioned at 90° intervals. In both cases, omnidirectional wheels equipped with passive rollers enable lateral motion relative to the drive direction. In four-wheel systems, Mecanum wheels are frequently used, allowing motors to be mounted in parallel and simplifying mechanical assembly. For the four-wheel configuration, several mathematical approaches exist to solve the inverse kinematics problem. These approaches rely on a transformation matrix that maps the desired velocity and rotation vector of the robot to individual motor velocities. In the standard 90° symmetric arrangement, this matrix exhibits structural properties that allow simplified analytical solutions. However, practical robotic platforms do not always maintain perfect symmetry. Compact layouts, structural constraints, or weight distribution requirements may lead to asymmetric wheel placement, where the front and rear wheel angles differ. In such cases, symmetric inverse-kinematics formulations are often applied beyond their validity range, potentially introducing systematic errors in motor commands and resulting motion. The objective of this paper is threefold. First, we derive an explicit analytical formulation for inverse kinematics in four-wheel omnidirectional robots with arbitrary wheel angles α and β. Second, we quantify the error introduced when symmetric-case equations are applied to asymmetric configurations. Third, we provide experimental validation on a real robotic platform to evaluate the practical impact of such kinematic approximations. The remainder of the paper is organized as follows. Section 2 reviews the related work. Section 3 recalls the three-wheel case for completeness. Section 4 presents the general four-wheel formulation. Section 5 evaluates the error induced by symmetric approximations. Section 6 reports the experimental validation. Section 7 discusses practical considerations and motor driving aspects. Section 8 concludes the paper.

***Corresponding author:** Raimondo Sgrò, IIS Cobianchi, Italy. Email: raimondo.sgro@cobianchi.it

© The Author(s) 2026. Published by BON VIEW PUBLISHING PTE. LTD. This is an open access article under the CC BY License (https://creativecommons.org/licenses/by/4.0/).

2. Related Work

Omnidirectional mobile robots have been extensively studied due to their ability to independently control planar translation and rotation. Foundational works such as Siegwart et al. [2] and Tagliavini et al. [3] provide comprehensive overviews of holonomic locomotion strategies and highlight the advantages of three- and four-wheel configurations. Early analytical treatments of omnidirectional kinematics [4] established closed-form solutions for symmetric layouts, particularly for three-wheel 120° arrangements and four-wheel 90° configurations. Subsequent research has addressed dynamic modeling and nonideal effects such as wheel slip and lateral sliding in omnidirectional robots [5]. Zeidis and Zimmermann [6] incorporate frictional interactions and full dynamic models for Mecanum-based systems. A recent systematic review of Mecanum and omni-wheel technologies is reported in Burkacki et al.'s study [7]. Slip estimation and compensation strategies have been investigated by Chen et al. [8], while control-oriented approaches are discussed in Comasolivas et al. [9], Al Mamun et al. [10], and Azizi et al.'s study [11], with recent model-predictive control strategies for Mecanum-wheeled robots [12]. These contributions primarily focus on symmetric wheel placements, where the transformation matrix exhibits structural properties that simplify analysis and control. Recent studies have also investigated wheel arrangements aimed at improving compactness in four-wheel omnidirectional platforms [13]. More recently, trajectory-tracking control for four-wheeled Mecanum platforms has been investigated in Hernández and Almeida's reaserch [14].

From a mathematical standpoint, inverse kinematics for omnidirectional robots can also be addressed using general linear-algebra tools, such as pseudo-inverse or least-squares formulations, particularly when the system is underdetermined. Such approaches provide numerical solutions for arbitrary configurations and are commonly embedded in control implementations. However, they often do not provide explicit analytical expressions tailored to specific geometric layouts, nor do they directly quantify the error introduced when symmetric-case assumptions are applied to asymmetric systems. Redundant robotic systems and the associated solution-space optimization problems have been extensively studied in the robotics literature [15].

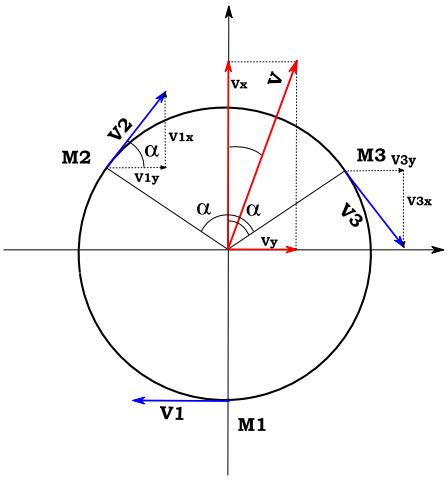
Although practical implementations with nonstandard wheel placements exist—particularly in compact or competition-oriented robots—explicit analytical treatments of asymmetric four-wheel configurations are rarely presented in a structured form. As a result, symmetric formulations are frequently extended beyond their original assumptions without systematic assessment of the resulting kinematic deviation. Preliminary observations on asymmetric wheel configurations were previously presented in Sgrò and Cacciatori's research [16].

The present work focuses specifically on this engineering scenario. Rather than proposing a new numerical solution method, it provides an explicit closed-form derivation for arbitrary wheel angles α and β, together with a quantitative evaluation of the error induced by symmetric approximations. This formulation aims to clarify the practical implications of asymmetric geometry in real robotic platforms.

3. Three-Wheel Case

The three-wheel configuration is the simplest holonomic arrangement. The inverse kinematics can be solved using basic trigonometric equations, without the need for matrix calculus. This provides an intuitive introduction to holonomic motion and inverse kinematics.

Figure 1
Three-wheel case: decomposition of the velocity components of the individual wheels and of the resulting velocity along the Cartesian axes



Referring to Figure 1, we can write two equations by decomposing the velocity into its components along the Cartesian axes. To solve it, we need a third equation, which can be obtained by imposing the constraint that the robot does not rotate. Obviously, it is also possible to introduce the rotation, but it requires using the cardinal equations of mechanics.

$$\begin{aligned} V_x &= V_2 \sin\alpha - V_3 \sin\alpha \\ V_y &= V_2 \cos\alpha - V_3 \cos\alpha - V_1 \\ 0 &= V_1 + V_2 + V_3 \end{aligned} \tag{1}$$

We can solve this system of three equations with three variables, in the case of = 60°:

$$\begin{aligned} V_1 &= -\frac{1}{1+\cos\alpha} V_y = -\frac{2}{3} V_y \\ V_2 &= \frac{1}{2\sin\alpha} V_x + \frac{1}{2(1+\cos\alpha)} V_y = \frac{1}{\sqrt{3}} V_x + \frac{1}{3} V_y \\ V_3 &= -\frac{1}{2\sin\alpha} V_x + \frac{1}{2(1+\cos\alpha)} V_y = -\frac{1}{\sqrt{3}} V_x + \frac{1}{3} V_y \end{aligned} \tag{2}$$

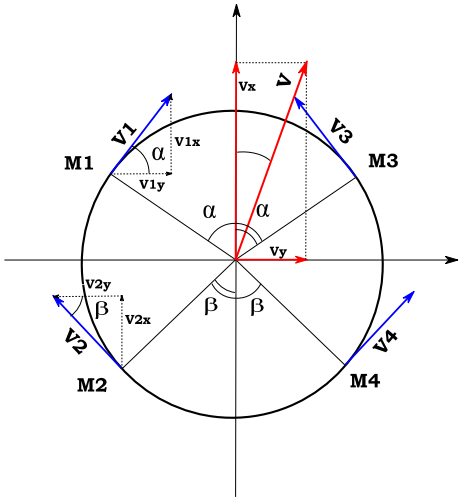
The three-wheel formulation also provides a useful structural reference for the four-wheel case. In particular, the four-motor configuration can be interpreted as an extension of the three-wheel system with one additional actuator, leading to an underdetermined linear system. Moreover, specific geometric choices of α and β reduce the general four-wheel formulation to configurations equivalent to the three-wheel case, as will be discussed in the following section. This connection clarifies the structural continuity between the two models.

4. Four-Wheel Case

The four-wheel configuration is intrinsically more complex. The system provides three independent equations but includes four unknown wheel velocities, leading to an underdetermined system unless additional constraints are introduced. According to Figure 2, we can write them as follows:

$$\begin{aligned} V_x &= V_1 \sin\alpha + V_2 \sin\beta + V_3 \sin\alpha + V_4 \sin\beta \\ V_y &= V_1 \cos\alpha - V_2 \cos\beta - V_3 \cos\alpha - V_4 \cos\beta \\ 0 &= V_1 + V_2 - V_3 - V_4 \end{aligned} \tag{3}$$

Figure 2
Four-wheel case: decomposition of the velocity components of the individual wheels and of the resulting velocity along the Cartesian axes. In this case, we observe the two angles α and β, referring to the alignment of the front and rear wheels, respectively



In this case, the solution is more complicated. The academic approach involves the use of matrix calculus. The issue, however, is that the matrix has dimensions 4 × 3, and since it is not square, it cannot be inverted.

It is convenient to write the system in matrix form

$$A\bar{x} = \bar{y},$$

where:

$$\bar{x} \equiv \begin{pmatrix} V_1 \\ V_2 \\ V_3 \\ V_4 \end{pmatrix}, \bar{y} \equiv \begin{pmatrix} V_x \\ V_y \\ 0 \end{pmatrix},$$
$$A \equiv \begin{pmatrix} \sin\alpha & \sin\beta & \sin\alpha & \sin\beta \\ \cos\alpha & -\cos\beta & -\cos\alpha & \cos\beta \\ 1 & 1 & -1 & -1 \end{pmatrix} \equiv \begin{pmatrix} W_1 \\ W_2 \\ W_3 \end{pmatrix} \quad (4)$$

In the symmetric case $\alpha = \beta$, the system simplifies because the vectors W_N become orthogonal. Therefore, we begin by analyzing this particular case. As previously mentioned, only square matrices are invertible, so we must work directly with the equations. To obtain a uniquely determined system, we introduce an additional linearly independent equation that allows the construction of a square matrix without imposing further physical constraints (see Appendix A). This extra equation is constructed to be orthogonal to the existing ones, allowing the resulting matrix to be orthogonal as well. Since an orthogonal matrix has the property that its inverse is equal to its transpose, we can easily compute the solution. In the case $\alpha = \beta$, the solution is (the most general solution, dependent on a free parameter p, is given in Appendix A):

$$\begin{aligned} V_1 &= \frac{1}{4\sin\alpha}V_x + \frac{1}{4\cos\alpha}V_y \\ V_2 &= \frac{1}{4\sin\alpha}V_x - \frac{1}{4\cos\alpha}V_y \\ V_3 &= \frac{1}{4\sin\alpha}V_x - \frac{1}{4\cos\alpha}V_y \\ V_4 &= \frac{1}{4\sin\alpha}V_x + \frac{1}{4\cos\alpha}V_y \end{aligned} \quad (5)$$

The factors 4 sin α and 4 cos α appear because the row vectors are not normalized to 1 but have norms 4 sin2 α, 4 cos2 α, and 4. What happens if we use the transpose in the general case $\alpha \neq \beta$ Taking into account that the norms of the row vectors are now 2(sin2 α + sin2 β), 2(cos2 α + cos2 β), and 4, we would get

$$\begin{aligned} V_1 &= \frac{\sin\alpha}{2(\sin^2\alpha + \sin\beta)}V_x + \frac{\cos\alpha}{2(\cos^2\alpha + \cos^2\beta)}V_y \\ V_2 &= \frac{\sin\beta}{2(\sin^2\alpha + \sin^2\beta)}V_x - \frac{\cos\beta}{2(\cos^2\alpha + \cos^2\beta)}V_y \\ V_3 &= \frac{\sin\alpha}{2(\sin^2\alpha + \sin^2\beta)}V_x - \frac{\cos\alpha}{2(\cos^2\alpha + \cos^2\beta)}V_y \\ V_4 &= \frac{\sin\beta}{2(\sin^2\alpha + \sin^2\beta)}V_x + \frac{\cos\beta}{2(\cos^2\alpha + \cos^2\beta)}V_y \end{aligned} \quad (6)$$

which reduces to Equation (5) for $\alpha = \beta$ but is not valid in the general asymmetric case.[1]

The four-wheel system, therefore, leads to an underdetermined linear problem, since three independent motion constraints are expressed in terms of four motor velocities. The associated transformation matrix is rectangular and cannot be inverted in the classical sense. While numerical approaches such as pseudo-inverse or least-squares formulations can provide general solutions for arbitrary configurations, our objective here is to derive an explicit analytical expression that highlights the geometric structure of the system and makes the dependence on the wheel angles α and β transparent.

In the asymmetric case ($\alpha \neq \beta$), the row vectors of the transformation matrix are no longer orthogonal. To obtain an explicit closed-form solution, we perform an orthogonalization procedure that preserves the original solution space while enabling the construction of a square invertible system. The detailed algebraic steps are reported in the Appendix for completeness. The resulting general solution is given by:

$$\begin{aligned} V_1 &= \frac{\sin\alpha}{2(\sin^2\alpha + \sin^2\beta)}V_x + \frac{1}{2(\cos\alpha + \cos\beta)}V_y \\ V_2 &= \frac{\sin\beta}{2(\sin^2\alpha + \sin^2\beta)}V_x - \frac{1}{2(\cos\alpha + \cos\beta)}V_y \\ V_3 &= \frac{\sin\alpha}{2(\sin^2\alpha + \sin^2\beta)}V_x - \frac{1}{2(\cos\alpha + \cos\beta)}V_y \\ V_4 &= \frac{\sin\beta}{2(\sin^2\alpha + \sin^2\beta)}V_x + \frac{1}{2(\cos\alpha + \cos\beta)}V_y \end{aligned} \quad (7)$$

The most general solution is presented in Appendix A.

We can observe that Equation (7) represents the general case. In fact, if we evaluate them for $\alpha = 60°$ and $\beta = 0°$, with appropriate adjustments to the directions and vectors, we obtain Equation (2). Naturally, we must consider that in the four-motor configuration, when $\beta = 0°$, both motors M2 and M4 in Figure 2 play the same role as M1 in Figure 1, and their power contribution should therefore be considered as half each.

$$\begin{aligned} V_1 &= \frac{1}{2\sin\alpha}V_x + \frac{1}{2(\cos\alpha + 1)}V_y \\ V_2 &= -\frac{1}{2(\cos\alpha + 1)}V_y \\ V_3 &= \frac{1}{2\sin\alpha}V_x - \frac{1}{2(\cos\alpha + 1)}V_y \\ V_4 &= \frac{1}{2(\cos\alpha + 1)}V_y \end{aligned}$$

[1] Since the second and third rows of the matrix are no longer orthogonal.

We can also make another consideration regarding the three-wheel case. If we rewrite Equation (1) in matrix form, we obtain:

$$A\bar{x} = \bar{y}$$
$$\mathrm{A} \equiv \begin{pmatrix} 0 & \sin\alpha & -\sin\alpha \\ -1 & \cos\alpha & \cos\alpha \\ 1 & 1 & 1 \end{pmatrix}$$

It is possible to calculate the determinant and thus compute the inverse matrix, as follows:

$$\det\mathrm{A} = 2\sin\alpha(1 + \cos\alpha) \neq 0 \leftrightarrow \alpha \neq 0$$
$$\mathrm{A}^{-1} \equiv \begin{pmatrix} 0 & -\frac{1}{1+\cos\alpha} & \frac{\cos\alpha}{2(1+\cos\alpha)} \\ \frac{1}{2\sin\alpha} & \frac{1}{2(1+\cos\alpha)} & \frac{1}{2(1+\cos\alpha)} \\ -\frac{1}{2\sin\alpha} & \frac{1}{2(1+\cos\alpha)} & \frac{1}{2(1+\cos\alpha)} \end{pmatrix}$$

so we can write:

$$\bar{\mathrm{x}} = \mathrm{A}^{-1}\bar{\mathrm{y}}$$

which corresponds to Equation (2). It is important to note that, since only W_1 and W_3 are orthogonal, the inverse matrix cannot be computed using the transpose method.

We are now interested in evaluating the magnitude of the error introduced by using the approximation Equation (6) in place of Equation (7).

5. Error Evaluation

A widely used formulation [4] for the symmetric configuration is often applied to asymmetric layouts, which we would like to compare with Equations (6) and (7). For clarity, it is reported below [4]:

$$\begin{aligned} \mathrm{V}_1 &= \sin\alpha\ \mathrm{V}_\mathrm{x} + \cos\alpha\ \mathrm{V}_\mathrm{y} \\ \mathrm{V}_2 &= \sin\beta\ \mathrm{V}_\mathrm{x} - \cos\beta\ \mathrm{V}_\mathrm{y} \\ \mathrm{V}_3 &= \sin\alpha\ \mathrm{V}_\mathrm{x} - \cos\alpha\ \mathrm{V}_\mathrm{y} \\ \mathrm{V}_4 &= \sin\beta\ \mathrm{V}_\mathrm{x} + \cos\beta\ \mathrm{V}_\mathrm{y} \end{aligned} \tag{8}$$

These equations are valid in the symmetrical case, but we would like to evaluate the error that occurs when they are applied to the asymmetric configuration, specifically for the case $\alpha = 55°$, $\beta = 45°$. The configuration $\alpha = 55°$, $\beta = 45°$ was selected as a representative asymmetric case corresponding to a practical robot layout, where moderate geometric deviation from symmetry is imposed by mechanical constraints.

To quantify the deviation introduced by simplified formulations, motor velocities are normalized such that $|\mathrm{V_i}| \leq 1$. The error for each motor is defined as

$$\Delta\mathrm{V_i} = \mathrm{V_i^{test}} - \mathrm{V_i^{ref}}$$

where $\mathrm{V_i^{ref}}$ is obtained from the general formulation (7) and $\mathrm{V_i^{test}}$ corresponds either to the symmetric-case expression (6) or to the classical RoboCup formulation (8). Since velocities are normalized, the magnitude of $\Delta\mathrm{V_i}$ can be directly interpreted as a percentage of the maximum motor command.

We begin by comparing Equations (7) and (8), obtaining the following errors:

As we can see, the errors are significant, which is expected since Equation (8) was derived under symmetry assumptions that do not hold in the present configuration. In particular, we can observe that the errors become zero only in the simple case where $\alpha = \beta = 45°$.

Next, we evaluate the error between formula (6), used in the general case (but valid only for $\alpha = \beta$), and Equation (7) for the same condition, $\alpha = 55°$, $\beta = 45°$

As we can see, the relative error reaches values as high as 9% in the case of a 90° displacement, which corresponds to the situation where the asymmetry between the two angles has the greatest impact. In this comparison as well, the errors become zero when $\alpha = \beta$.

The motor-level deviation propagates to the resulting planar velocity components V_x and V_y, which are linear combinations of the individual wheel velocities. Let the vector of wheel velocities be denoted as $\mathrm{V} = [\mathrm{V_1}, \mathrm{V_2}, \mathrm{V_3}, \mathrm{V_4}]^\mathrm{T}$. The planar velocity components can be expressed as a linear transformation

$$\mathrm{v_{xy}} = \begin{pmatrix} \mathrm{V_x} \\ \mathrm{V_y} \end{pmatrix} = \mathrm{AV},$$

where A is the kinematic transformation matrix derived in Section 4. Consequently, motor-level deviations $\Delta\mathrm{V}$ induce corresponding variations in the planar velocity components given by

$$\Delta\mathrm{v_{xy}} = \mathrm{A}$$

The resulting heading angle is defined as θ = archant $2(\mathrm{V_Y}, \mathrm{V_X})$ For small perturbations, the corresponding angular deviation can be approximated as

$$\Delta\theta \approx \frac{\mathrm{V_x}\Delta\mathrm{V_y} - \mathrm{V_y}\Delta\mathrm{V_x}}{\mathrm{V_x^2} + \mathrm{V_y^2}}.$$

This expression shows that even moderate motor-level discrepancies may translate into measurable heading errors, particularly when the robot operates at low translational speed (i.e., when $\mathrm{V_x^2} + \mathrm{V_y^2}$ is small) or when the deviation acts orthogonally to the intended motion direction. Therefore, the heading deviation ultimately originates from the motor-level discrepancies quantified in Tables 1 and 2.

The induced heading deviation can be approximated by a first-order expansion (see Appendix B).

Table 1
Error evaluation between Equations (7) and (8)

Direction	V1	V2	V3	V4
0	0, 12	0, 10	–0, 12	–0, 10
15	0, 06	0, 12	–0, 17	–0, 08
30	0, 00	0, 13	–0, 21	–0, 05
45	–0, 06	0, 13	–0, 23	–0, 02
60	–0, 12	0, 12	–0, 24	0, 01
90	–0, 21	0, 07	–0, 21	0, 07

Table 2
Error evaluation between Equations (6) and (7)

Direction	V1	V2	V3	V4
0	0, 00	0, 00	0, 00	0, 00
15	–0, 02	–0, 02	–0, 02	–0, 02
30	–0, 04	–0, 04	–0, 04	–0, 04
45	–0, 06	–0, 05	–0, 06	–0, 05
60	–0, 08	–0, 06	–0, 08	–0, 06
90	–0, 09	–0, 07	–0, 09	–0, 07

6. Experimental Validation

6.1. Experimental setup

Experimental tests were conducted on a four-wheel omnidirectional platform configured with asymmetric wheel angles $\alpha = 55°$ and $\beta = 45°$. The system operates in open-loop mode, with motor commands normalized in the range $[-1, 1]$, consistent with the analytical model. A calibrated motor activation offset is implemented in the firmware to compensate for static friction effects and ensure consistent motor engagement (see Appendix C).

The available test field provided a maximum longitudinal distance of 2.30 m. Accounting for the robot footprint (0.20 m), the effective travel distance was set to 2.10 m for all trials. For each target steering angle, the robot was commanded to move along a straight trajectory starting from a fixed reference point. The final position (x_f, y_f) was measured relative to the origin using ground reference markings. The effective motion direction was computed as

$$\theta_{meas} = \arctan 2(y_f, x_f).$$

This approach provides a direct geometric evaluation of heading deviation without relying on encoder-based odometry, thereby isolating the purely kinematic effects of the inverse-kinematics formulation. Similar heading-correction problems have been observed in industrial omnidirectional robots [17].

6.2. Test protocol

Experimental validation focused on two representative steering angles, 15° and 30°, selected due to their sensitivity to asymmetric geometric configurations, as suggested by the analytical error propagation model discussed in the previous sections. Four repeated trials were performed for each steering angle and each kinematic formulation. The heading error was defined as

$$\Delta\theta = \theta_{meas} - \theta_{target}.$$

For each condition, the mean absolute error (MAE) and standard deviation were computed. The experimental comparison was performed between:

The classical RoboCup symmetric formulation, and the proposed asymmetric analytical formulation is derived in Section 4.

6.3. Results and discussion

For the 15° target angle, the RoboCup formulation produced a mean heading error of approximately 5°, whereas the proposed asymmetric formulation reduced the error to approximately 3°. The discrepancy becomes significantly more pronounced at 30°. In this case, the symmetric RoboCup formulation resulted in a systematic deviation exceeding 16° on average, while the proposed analytical solution limited the error to approximately 2–3°. Table 3 reports the mean measured heading angle, standard deviation, and MAE for both formulations. The relatively small standard deviations observed across all trials indicate that the deviation is systematic rather than random, supporting the interpretation that the error originates from structural kinematic inconsistency rather than experimental noise.

Overall, the experimental results confirm the analytical findings: applying symmetric inverse-kinematics formulations to asymmetric wheel configurations introduces measurable directional errors, whereas the proposed general formulation significantly improves motion fidelity. The mean measured angle corresponds to the average final heading direction of the robot measured with respect to the reference trajectory.

7. Practical Considerations

When comparing two-, three-, and four-wheel holonomic drive systems, we can observe that each configuration presents some "natural" movement directions—by this, we mean directions where certain wheel speeds V_N can be set to zero or fixed values. In the two-wheel case, the natural directions are forward and backward (i.e., $\theta = 0°$ and $\theta = 180°$), along with the basic turning motions (left/right rotation).

In the three-wheel setup, natural movement directions typically occur at angles that are multiples of 60°, while in the four-wheel symmetrical configuration, they occur at multiples of 45°. These natural directions are useful for introducing omnidirectional drive through basic experiments. Once these basics are understood, the next step is implementing movement in arbitrary directions. In this case, several key factors must be taken into account:

1) Wheel design
2) Surface properties
3) Motor driver's transfer function

Omnidirectional movement assumes that the robot's resulting direction is the vector sum of the individual wheel velocities. However, this vector sum is physically realized through the interaction of the wheels with the floor surface. Omnidirectional wheels must therefore be designed to both transmit traction in the drive direction and allow lateral slip to discharge orthogonal velocity components.

The two common types of wheels used in holonomic systems are Mecanum and omni wheels. In both cases, the discharge direction is orthogonal to the main traction axis, which fits well in symmetrical configurations. In asymmetric layouts, however, special care must be taken in selecting or designing wheels so that they properly handle the force distribution and motion vectors. Additionally, the floor surface influences the choice of materials for wheel construction—grip, friction, and compliance all matter.

Table 3
Experimental heading deviation for RoboCup and proposed asymmetric formulation (x = 2.10 m, 4 trials per condition)

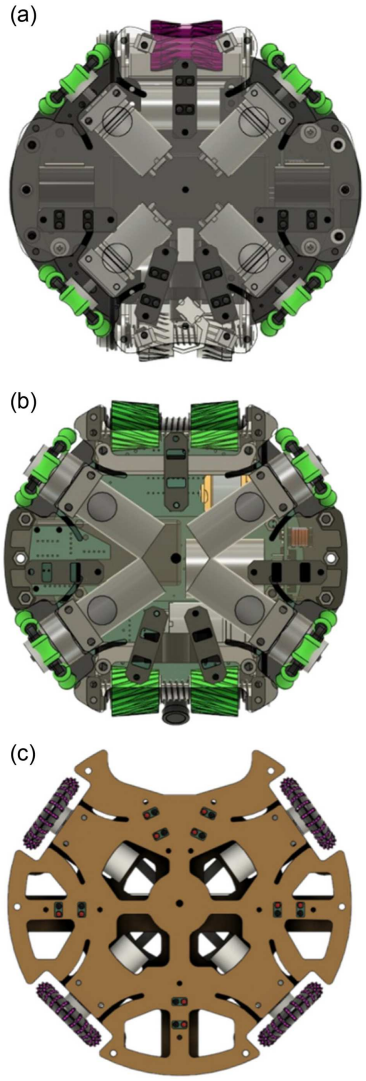
Target angle (°)	Formulation	Mean measured angle (°)	Std dev (°)	Mean absolute error (°)
15	RoboCup	9.86	0.76	5.14
15	Proposed	12.09	0.30	2.91
30	RoboCup	13.78	0.54	16.22
30	Proposed	27.54	0.67	2.46

The proposed formulation is purely kinematic and assumes ideal rolling conditions. In real systems, dynamic effects, friction, wheel slip, and locomotion over uneven terrain may influence the actual motion of the platform [18]. These aspects are not explicitly modeled in this work and may be considered in future developments. These aspects are not explicitly modeled in this work and may be considered in future developments. Additional details regarding the motor driving strategy adopted during the experiments are reported in Appendix C. Figure 3 shows different wheel-angle configurations for four-wheel RoboCup Junior robots, while Figure 4 presents examples of Mecanum and omnidirectional wheel designs.

We now analyze the motor load distribution in both three- and four-wheel configurations. If we plot Equations (2) and (7), we obtain the following graphs:

If we examine Figures 5 and 6, we can see that in the three-wheel configuration, the load on the three motors is a periodic function of the motion direction, with each motor shifted by 120°.

Figure 3
Comparison between (a) a symmetric 45° configuration, (b) 55° case, and (c) asymmetric configuration with 55°–45° case in a RoboCup junior soccer robot[2]



[2] https://junior.robocup.org/soccer/

Figure 4
(a) 3D model of a Mecanum wheel and (b) omni-drive wheel

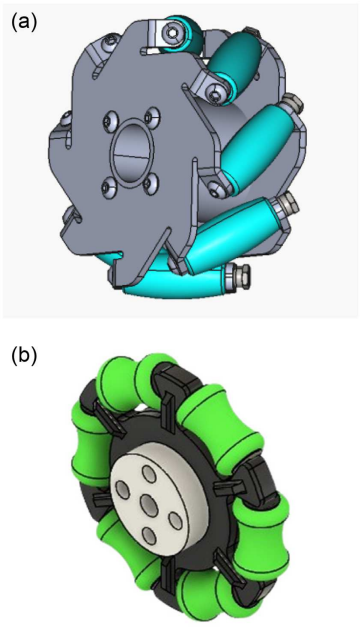


Figure 5
The trend of the motor speeds and of the average speeds in the three-wheel case, as a function of the direction

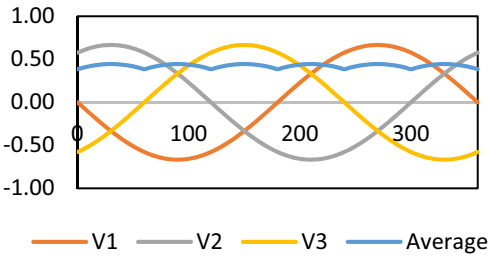
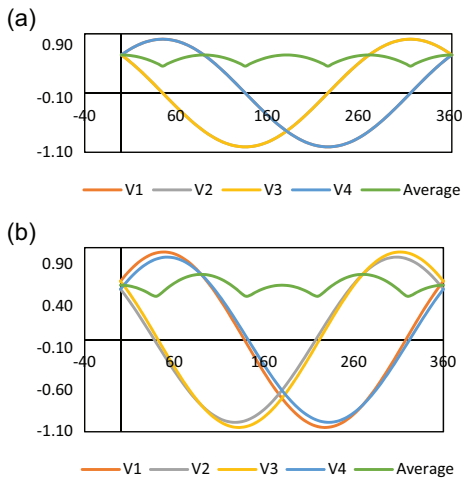


Figure 6
The trend of the motor speeds and of the average speeds in the four-wheel case, as a function of the direction, in case of (a) $\alpha = \beta = 45°$ and (b) $\alpha = 55°$, $\beta = 45°$



In the symmetric four-wheel configuration, the situation is similar, but symmetry causes the motors to appear in symmetric pairs, with a phase shift of 90° between the pairs. In the asymmetric case, however (Figure 6(b)), this symmetry is lost.

8. Conclusions

This work addressed the inverse-kinematics formulation of four-wheel omnidirectional robots under asymmetric wheel configurations, where the front and rear wheel angles differ. While symmetric arrangements admit simplified analytical solutions, their direct application to asymmetric geometries may introduce systematic kinematic deviations. An explicit closed-form inverse-kinematics formulation valid for arbitrary angles α and β was derived using a structured linear-algebra approach. The analytical comparison demonstrated that extending symmetric formulations beyond their intended configuration may lead to non-negligible motor-level discrepancies. The subsequent error propagation analysis showed that such discrepancies directly affect the resulting heading angle. Experimental validation on a real robotic platform configured with $\alpha = 55°$ and $\beta = 45°$ confirmed the theoretical findings. In particular, the symmetric RoboCup formulation produced significant directional deviation at 30°, whereas the proposed asymmetric formulation maintained substantially lower heading error. These results highlight the importance of adopting geometry-consistent kinematic models when symmetry assumptions cannot be maintained. The proposed formulation provides a practical and analytically grounded solution for compact omnidirectional robots operating under asymmetric design constraints. Future work will extend the experimental validation to additional steering angles and investigate the integration of the proposed formulation within closed-loop control architectures.

Ethical Statement

This study does not contain any studies with human or animal subjects performed by any of the authors.

Conflicts of Interest

The authors declare that they have no conflicts of interest to this work.

Data Availability Statement

Data are available from the corresponding author upon reasonable request.

Author Contribution Statement

Raimondo Sgrò: Conceptualization, Software, Validation, Investigation, Resources, Data curation, Writing – original draft, Writing – review & editing, Visualization, Project administration. **Sergio Cacciatori:** Methodology, Validation, Formal analysis, Writing – original draft, Writing – review and editing.

References

[1] Loganathan, A., & Ahmad, N. S. (2023). A systematic review on recent advances in autonomous mobile robot navigation. *Engineering Science and Technology, an International Journal*, *40*, 101343. https://doi.org/10.1016/j.jestch.2023.101343

[2] Siegwart, R., Nourbakhsh, I. R., & Scaramuzza, D. (2011). *Introduction to autonomous mobile robots* (2nd ed.). The MIT Press.

[3] Tagliavini, L., Colucci, G., Botta, A., Cavallone, P., Baglieri, L., & Quaglia, G. (2022). Wheeled mobile robots: State of the art overview and kinematic comparison among three omnidirectional locomotion strategies. *Journal of Intelligent & Robotic Systems*, *106*(3), 57. https://doi.org/10.1007/s10846-022-01745-7

[4] Rojas, R. (2005). *Omnidirectional control*. Freie Universität Berlin. http://robocup.mi.fu-berlin.de/buch/omnidrive.pdf

[5] Bárcenas-Presteguí, C. B., Velasco-Villa, M., González-Sierra, J., & Aguilar-Pérez, J. I. (2025). Kinematic modeling and control of an omnidirectional mobile robot subject to wheel slippage and lateral and longitudinal sliding. *Control Theory and Technology*, *23*(3), 410–422. https://doi.org/10.1007/s11768-025-00269-3

[6] Zeidis, I., & Zimmermann, K. (2019). Dynamics of a four-wheeled mobile robot with Mecanum wheels. *ZAMM-Journal of Applied Mathematics and Mechanics*, *99*(12), e201900173. https://doi.org/10.1002/zamm.201900173

[7] Burkacki, M., Łysy, I., Suchoń, S., Chrzan, M., & Kowolik, R. (2025). Systematic review of Mecanum and omni wheel technologies for motor impairments. *Applied Sciences*, *15*(9), 4773. https://doi.org/10.3390/app15094773

[8] Chen, P.-J., Yang, S.-Y., Chen, Y.-P., Muslikhin, M., & Wang, M.-S. (2021). Slip estimation and compensation control of omnidirectional wheeled automated guided vehicle. *Electronics*, *10*(7), 840. https://doi.org/10.3390/electronics10070840

[9] Comasolivas, R., Quevedo, J., Escobet, T., Escobet, A., & Romera, J. (2015). Low level control of an omnidirectional mobile robot. In *2015 23rd Mediterranean Conference on Control and Automation*, 1160–1166. https://doi.org/10.1109/MED.2015.7158912

[10] Al Mamun, M. A., Nasir, M. T., & Khayyat, A. (2018). Embedded system for motion control of an omnidirectional mobile robot. *IEEE Access*, *6*, 6722–6739. https://doi.org/10.1109/ACCESS.2018.2794441

[11] Azizi, M. R., Rastegarpanah, A., & Stolkin, R. (2021). Motion planning and control of an omnidirectional mobile robot in dynamic environments. *Robotics*, *10*(1), 48. https://doi.org/10.3390/robotics10010048

[12] Moreno-Caireta, I., Celaya, E., & Ros, L. (2021). Model predictive control for a Mecanum-wheeled robot navigating among obstacles. *IFAC-PapersOnLine*, *54*(6), 119–125. https://doi.org/10.1016/j.ifacol.2021.08.533

[13] Hijikata, M., Miyagusuku, R., & Ozaki, K. (2022). Wheel arrangement of four omni wheel mobile robot for compactness. *Applied Sciences*, *12*(12), 5798. https://doi.org/10.3390/app12125798

[14] Hernández, J. C. O., & Almeida, D. I. R. (2024). Kinematic control in a four-wheeled Mecanum mobile robot for trajectory tracking. *The Journal of Engineering*, *2024*(9), e70006. https://doi.org/10.1049/tje2.70006

[15] Nakamura, Y. (1991). *Advanced robotics: Redundancy and optimization*. Addison-Wesley.

[16] Sgrò, R., & Cacciatori, S. (2025). *Omnidirectional drive in junior leagues: Asymmetric configuration* [Conference presentation]. Workshop on Educational Robotics, Salvador, Brazil. https://2025.robocup.org/werob/

[17] Galati, R., Mantriota, G., & Reina, G. (2022). Adaptive heading correction for an industrial heavy-duty omnidirectional

robot. *Scientific Reports*, *12*(1), 19608. https://doi.org/10.1038/s41598-022-24270-x

[18] Nodehi, S. (2023). *Locomotion system for ground mobile robots in uneven and unstructured environments* [Doctoral dissertation, University of Genoa]. UNITesi. https://hdl.handle.net/20.500.14242/67085

[19] Sgrò, R. (2021). *Guida al progetto di un robot: Per l'hobbista e lo studente* [Robot design guide: For hobbyists and students]. Sandit Libri.

[20] Patel, A. (2025). Low-cost DC motor design for embedded systems in smart applications. *Journal Innovations Computer Science*, *4*(2), 165–176. https://doi.org/10.56347/jics.v4i2.273

How to Cite: Sgrò, R., & Cacciatori, S. (2026). Asymmetric Configuration for a Four-Motor Omnidirectional Robot. *Archives of Advanced Engineering Science*, *4*(4), 411–422. https://doi.org/10.47852/bonviewAAES62028258

Appendix A – Orthogonalization Procedure for the Asymmetric Four-Wheel System

To solve system (4), we introduce a fictitious equation that renders the system uniquely determined without adding constraints. A vector orthogonal to W_1, W_2, and W_3 is defined, forming an orthonormal basis. For $\alpha \neq \beta$, W_2 is orthogonalized by subtracting its projection on W_3. The resulting matrix becomes orthogonal and is inverted through transposition, yielding Equation (7).

Let us first consider the case when $\alpha = \beta$ and introduce the vector:

$$W_4 = \frac{1}{2}(1, -1, 1, -1) \tag{9}$$

It is normalized and orthogonal to W_N, N=1, 2, 3, so together with such vectors it determines an orthonormal basis. We then add the equation

$$\frac{1}{2}\,(V_1 - V_2 + V_3 - V_4) = p \tag{10}$$

This is a fictitious equation in the sense that we do not fix p a priori. In other words, we add to the original system a fourth equation independent of the first three. This is obtained by taking an independent linear combination of the xj, j = 1, . . . , 4, that we put equal to "whatever" (that we call p). It is clear that this does not affect the previous system and, rather, it allows us to find all possible solutions by leaving p to change freely. Moreover, the final system doesn't depend on the explicit choice of the fourth equation, as long as it is linearly independent from the others. Therefore, the best way to choose it is to take it orthonormal to the previous lines, as we did, so as to form an orthogonal matrix $\widetilde{A}$. We can therefore rewrite (4) as follows:

$$\widetilde{A}\bar{x} = \bar{y}. \tag{11}$$

Explicitly:

$$\begin{pmatrix} \frac{1}{2} & \frac{1}{2} & \frac{1}{2} & \frac{1}{2} \\ \frac{1}{2} & -\frac{1}{2} & -\frac{1}{2} & \frac{1}{2} \\ \frac{1}{2} & \frac{1}{2} & -\frac{1}{2} & -\frac{1}{2} \\ \frac{1}{2} & -\frac{1}{2} & \frac{1}{2} & -\frac{1}{2} \end{pmatrix} \begin{pmatrix} V_1 \\ V_2 \\ V_3 \\ V_4 \end{pmatrix} = \begin{pmatrix} \frac{V_x}{2\sin\alpha} \\ \frac{V_y}{2\cos\alpha} \\ 0 \\ p \end{pmatrix}. \tag{12}$$

The advantage is that now $\widetilde{A}$ is a 4×4 invertible matrix. In the case $\alpha = \beta$ it is orthogonal, so its inverse is simply its transpose, $\widetilde{A}^{-1} = \widetilde{A}^{t}$

$$\bar{x} = \widetilde{A}^{t}\bar{y} \tag{13}$$

that is

$$\begin{pmatrix} V_1 \\ V_2 \\ V_3 \\ V_4 \end{pmatrix} = \begin{pmatrix} \frac{1}{2} & \frac{1}{2} & \frac{1}{2} & \frac{1}{2} \\ \frac{1}{2} & -\frac{1}{2} & \frac{1}{2} & -\frac{1}{2} \\ \frac{1}{2} & -\frac{1}{2} & -\frac{1}{2} & \frac{1}{2} \\ \frac{1}{2} & \frac{1}{2} & -\frac{1}{2} & -\frac{1}{2} \end{pmatrix} \begin{pmatrix} \frac{V_x}{2\sin\alpha} \\ \frac{V_y}{2\cos\alpha} \\ 0 \\ p \end{pmatrix}. \tag{14}$$

In components, these are

$$\begin{aligned} V_1 &= \frac{V_x}{4\sin\alpha} + \frac{V_y}{4\cos\alpha} + \frac{p}{2} \\ V_2 &= \frac{V_x}{4\sin\alpha} - \frac{V_y}{4\cos\alpha} - \frac{p}{2} \\ V_3 &= \frac{V_x}{4\sin\alpha} - \frac{V_y}{4\cos\alpha} + \frac{p}{2} \\ V_4 &= \frac{V_x}{4\sin\alpha} + \frac{V_y}{4\cos\alpha} - \frac{p}{2} \end{aligned}$$

and choosing $p = 0$, we obtain Equation (5). However, we remark that for every given p, we have a solution of the system (3) when $\alpha = \beta$.

-Remark: We also note that the third column of the matrix multiplies 0 and could be dropped. Nevertheless, it is interesting to keep it in case one would need to solve the same problem with a nonzero rotation.

In the case $\alpha \neq \beta$, however, the rows of the original system are not orthogonal, and we do not get an orthogonal matrix. Nevertheless, we can make them orthogonal by subtracting from W_2 its projection on W_3. This projection is $\frac{\cos\alpha - \cos\beta}{2} W_3$, so we can replace W_2 with

$$\widetilde{W_2} = W_2 - \frac{\cos\alpha - \cos\beta}{2} W_3 = (\cos\alpha + \cos\beta)\tilde{n}_2$$

where $\tilde{n}_2 = \frac{1}{2}(1, -1, -1, 1)$. Notice that this is a linear operation on the rows, so we should do the same operations on the right-hand side of the equation. However, since in our specific case y3 = 0, this does not affect the r.h.s. of the equations.

We need to bring the equation back to the previous orthonormal case, allowing us to apply the same method of adding a fourth vector. In this case, the normalized vector orthogonal to the first three rows is:

$$W_4 = \frac{1}{\sqrt{2\left(\sin^2\alpha + \sin^2\beta\right)}}(\sin\beta, -\sin\alpha, \sin\beta, -\sin\alpha). \tag{15}$$

Correspondingly, as above, we add a fourth fictitious equation $W_4\bar{x} = p$. It is then convenient to introduce the normalized vectors $\tilde{n}_j$ for j = 1, 3, 4, defined by

$$W_1 = \sqrt{2\left(\sin^2\alpha + \sin^2\beta\right)}\tilde{n}_1,$$

$$\tilde{n}_3 = \frac{1}{2}(1, 1, -1, -1),$$

and $\tilde{n}_4 = W_4$. If we divide each row by the coefficient of $\tilde{n}_j$, we have to do the same in the l.h.s. In this way, we can rewrite the linear system in the form:

$$\begin{pmatrix} \tilde{n}_1 \\ \tilde{n}_2 \\ \tilde{n}_3 \\ \tilde{n}_4 \end{pmatrix} \bar{x} \equiv \begin{pmatrix} \frac{V_x}{\sqrt{2(\sin^2\alpha + \sin^2\beta)}} \\ \frac{V_y}{(\cos\alpha + \cos\beta)} \\ 0 \\ p \end{pmatrix}, \tag{16}$$

which is easily invertible, since the matrix is now orthogonal. By multiplying by the transpose and choosing $p = 0$, we obtain Equation (7). More in general, for $p \neq 0$, we get

$$\begin{pmatrix} V_1 \\ V_2 \\ V_3 \\ V_4 \end{pmatrix} = \begin{pmatrix} \frac{\sin\alpha}{\sqrt{2(\sin^2\alpha + \sin^2\beta)}} & \frac{1}{2} & \frac{1}{2} & \frac{\sin\beta}{\sin\beta} \\ \frac{\sin\beta}{\sqrt{2(\sin^2\alpha + \sin^2\beta)}} & -\frac{1}{2} & \frac{1}{2} & -\frac{\sin\alpha}{\sqrt{2(\sin^2\alpha + \sin^2\beta)}} \\ \frac{\sin\alpha}{\sqrt{2(\sin^2\alpha + \sin^2\beta)}} & -\frac{1}{2} & -\frac{1}{2} & \frac{\sin\beta}{\sqrt{2(\sin^2\alpha + \sin^2\beta)}} \\ \frac{\sin\beta}{\sqrt{2(\sin^2\alpha + \sin^2\beta)}} & \frac{1}{2} & -\frac{1}{2} & -\frac{\sin\alpha}{\sqrt{2(\sin^2\alpha + \sin^2\beta)}} \end{pmatrix} \begin{pmatrix} \frac{V_x}{\sqrt{2(\sin^2\alpha + \sin^2\beta)}} \\ \frac{V_y}{(\cos\alpha + \cos\beta)} \\ 0 \\ p \end{pmatrix}. \tag{17}$$

In components, we get

$$\begin{aligned} V_1 &= \frac{\sin\alpha V_x}{2(\sin^2\alpha + \sin^2\beta)} + \frac{V_y}{2(\cos\alpha + \cos\beta)} + \frac{\sin\beta\ p}{\sqrt{2(\sin^2\alpha + \sin^2\beta)}} \\ V_2 &= \frac{\sin\beta V_x}{2(\sin^2\alpha + \sin^2\beta)} - \frac{V_y}{2(\cos\alpha + \cos\beta)} - \frac{\sin\alpha\ p}{\sqrt{2(\sin^2\alpha + \sin^2\beta)}} \\ V_3 &= \frac{\sin\alpha V_x}{2(\sin^2\alpha + \sin^2\beta)} - \frac{V_y}{2(\cos\alpha + \cos\beta)} + \frac{\sin\beta\ p}{\sqrt{2(\sin^2\alpha + \sin^2\beta)}} \\ V_4 &= \frac{\sin\beta V_x}{2(\sin^2\alpha + \sin^2\beta)} + \frac{V_y}{2(\cos\alpha + \cos\beta)} - \frac{\sin\alpha\ p}{\sqrt{2(\sin^2\alpha + \sin^2\beta)}} \end{aligned}$$

This provides the most general solution of system (3). Choosing $p = 0$ gives (7). By varying p, we get all possible solutions.

Appendix B – First-Order Propagation of Heading Error

The heading angle of the robot is defined as

$$\theta = \arctan 2(V_y, V_x),$$

where V_x and V_y are the planar velocity components resulting from the wheel velocities.

To evaluate the influence of motor-level deviations on the heading angle, consider small perturbations ΔV_x and ΔV_y. A first-order Taylor expansion yields

$$\Delta\theta \approx \frac{\partial\theta}{\partial V_x}\Delta V_x + \frac{\partial\theta}{\partial V_y}\Delta V_y.$$

Using the known partial derivatives of the atan2 function,

$$\frac{\partial\theta}{\partial V_x} = -\frac{V_y}{V_x^2 + V_y^2}, \frac{\partial\theta}{\partial V_y} = \frac{V_x}{V_x^2 + V_y^2}$$

we obtain

$$\Delta\theta \approx \frac{V_x\Delta V_y - V_y\Delta V_x}{V_x^2 + V_y^2}.$$

This expression shows that heading sensitivity depends on both the direction of motion and the magnitude of the translational velocity.

Appendix C – Motor Driving

Another critical factor is the motor driver's transfer function; in fact, when calculating normalized speed values, we often assume that the motor's response is linear with respect to the Pulse Width Modulation (PWM) signal (0–100%). If we decide to use a DC motor, for example, the relationship between angular velocity and applied voltage is linear but does not pass through the origin. This means a voltage offset is needed to overcome static friction and load torque before the motor starts rotating. The relationship can be expressed as:

$$\omega = \frac{V_a}{K_E} - C_M \frac{R_a}{K_T K_E}$$

Where:

CM: mechanical torque
Ra: motor resistance
Va: applied voltage
KT: torque constant
KE: angular velocity constant
ω: angular velocity

This relationship [19] refers to the stationary regime, where inductive and inertial transient effects are negligible. Similar simplified DC motor models are commonly adopted in embedded motor-control applications [20]. It is worth noting that the relationship between PWM duty cycle and angular velocity describes the average steady-state behavior of the motor and does not include transient effects such as current rise, inductive delays, or torque ripple.

We are therefore faced with two possibilities:

- Use an open-loop control system
- Use a closed-loop control system

In the first case, we must consider the motor's actual transfer function linking angular velocity and voltage. This means that with $CM \neq 0$, the motor requires a minimum voltage to begin moving—this corresponds to a nonzero offset in software. A practical way to account for this is to experimentally determine a small constant value that is subtracted or added to the PWM signal to ensure the motor starts reliably. In the second case, the assumption of a linear relationship between the PWM signal and motor speed can be considered true, as the property of feedback systems to reduce nonlinearities is known. To implement such a system, however, it is necessary to use motors with encoders and a control system for each motor, increasing the complexity of the system.